



## Test beam results on the ATLAS liquid argon electromagnetic calorimeter

L. Di Ciaccio

### ► To cite this version:

L. Di Ciaccio. Test beam results on the ATLAS liquid argon electromagnetic calorimeter. International Europhysics Conference on High Energy Physics EPS 2003, Jul 2003, Aachen, Germany. pp.s1005 - s1007, 10.1140/epjcd/s2004-03-1796-6 . in2p3-00014165

**HAL Id: in2p3-00014165**

**<https://hal.in2p3.fr/in2p3-00014165>**

Submitted on 25 Nov 2003

**HAL** is a multi-disciplinary open access archive for the deposit and dissemination of scientific research documents, whether they are published or not. The documents may come from teaching and research institutions in France or abroad, or from public or private research centers.

L'archive ouverte pluridisciplinaire **HAL**, est destinée au dépôt et à la diffusion de documents scientifiques de niveau recherche, publiés ou non, émanant des établissements d'enseignement et de recherche français ou étrangers, des laboratoires publics ou privés.

LAPP-EXP 2003-23  
November 2003

**Test beam results on the ATLAS liquid argon electromagnetic calorimeter**

**L. Di Ciaccio**

On behalf of ATLAS Collaboration

LAPP-IN2P3-CNRS  
9 chemin de Bellevue - BP. 110  
F-74941 Annecy-le-Vieux Cedex

**Presented at the International Europhysics Conference on  
High Energy Physics EPS, Aachen, Germany, July 17-23, 2003**

# Test Beam Results on the ATLAS Electromagnetic Calorimeter

Lucia Di Ciaccio

on behalf of the ATLAS Liquid Argon calorimeters group

LAPP, CNRS-IN2P3-Université de Savoie

Chemin de Bellevue, BP110 74941 Annecy-le-Vieux CEDEX, France

e-mail: lucia.di.ciaccio@cern.ch

Received: xx / Revised version: xx

**Abstract.** ATLAS, one of the two multi-purpose detectors at the proton-proton collider LHC, will start taking physics data in 2007. The construction of its electromagnetic calorimeter is well advanced and modules of the barrel and end-cap parts have been tested under electron beams at CERN. Results on energy resolution, uniformity of the energy response, position and time resolution are presented.

**PACS.** XX.XX.XX No PACS code given

## 1 Introduction

The ATLAS detector has been mainly designed to search for new particles related to the symmetry breaking mechanism. The physics program includes also precise measurements of known objects like W, t and b particles [1]. The electromagnetic calorimetry plays an essential role since electron identification, photon reconstruction, jet and missing energy measurements are the fundamental tasks for such studies. Excellent performances in terms of energy resolution and response uniformity are required in particular at hadron colliders where the number of physics background events is high and the beam energy constraint can be applied only in the plane transverse to the beam direction. Furthermore at LHC, detection has to be carried out in an environnement with high collision rate and high radiation level background. The ATLAS electromagnetic calorimeter is based on a lead-liquid argon sampling technique which guarantees intrinsic linear behaviour, stability of the response and radiation hardness [2]. The accordion geometry of the electrodes and of the absorbers avoids uninstrumented areas in the azimuthal angle  $\phi$ . The calorimeter has high granularity ( $\approx 2 \times 10^5$  channels) and the associated electronics has been designed to have fast response and wide dynamic range. Test beam measurements are extremely important to check that the final modules meet the requirements for the LHC physics. Recent results of these tests are presented in Sect. 3 of this paper, after a brief description of the calorimeter.

## 2 The ATLAS Electromagnetic Calorimeter

The calorimeter [2] is made of two half-barrels ( $|\eta| \leq 1.475$ ) and two end-cap wheels ( $1.375 \leq |\eta| \leq 3.2$ ). Each barrel part is composed of 16 modules, one module covering

a region  $\Delta\eta \times \Delta\phi = 1.475 \times (2\pi/16)$ . A module has 3 compartments in depth: the first one ('front') highly segmented in  $\eta$  for  $\gamma/\pi^0$  separation, the second ('middle') where the main energy deposition occurs and the third ('back') to help in disentangling electromagnetic from hadronic showers. In front of the calorimeter a presampler detector ( $|\eta| \leq 1.8$ ) also based on a lead-liquid argon technique, allows to correct for the energy loss due to dead material. Each end-cap wheel is formed of 8 modules with similar structure to the barrel modules. Differently from the barrel module gaps, the liquid argon gaps of the end-cap modules increase with radius. To keep the detector response independent of  $\eta$ , the high voltage across the gaps should be varied accordingly in a continuous way. In practice to make operation easier, the high voltage is varied in 9  $\eta$  steps.

At the time of these proceedings the two half-barrels and one of end-cap wheel have been assembled, inserted in the cryostat and tested.

## 3 Test Beam Results

Two full-size prototype modules[3] (one barrel, one end-cap) and seven production modules (four barrel modules, three end-cap modules) have been tested with electron beams at the CERN H8 facility. Many topics have been studied including linearity,  $\gamma/\pi^0$  separation, response to muons, noise and cross-talk. This section, after a brief description of the procedure to compute the electron energy in test beam data, presents some of the important performances like energy resolution, uniformity of the energy response, position and time resolutions.

### 3.1 Electron Energy Reconstruction

A read-out electronics very close to the final one has been used. The ionization signal from each channel is amplified, shaped, sampled every 25 ns and digitized. Five samples are recorded. Each digitized sample,  $S_i$ , is converted in GeV using a calibration procedure based on injecting very precise current pulses in each read-out channel and the knowledge of the energy deposited in liquid and of the sampling fraction. To estimate the signal height, representing the calibrated cell energy, an optimal filtering technique (OF) [4] is used ( $E_{\text{cell}} = \sum_i a_i S_i$ ) which minimizes pile-up and noise. The OF coefficients,  $a_i$ , are computed from the physics signal shapes and the noise autocorrelation matrix. The physics signal shapes are predicted using the calibration signal shapes corrected for the different input currents and injection points in physics and calibration runs. With the current procedure the relative difference between the predicted and the measured physics signals in every time bin of 1 ns is at most 1%. After the reconstruction of  $E_{\text{cell}}$ , clusters of cells are built around the most energetic one in the presampler and in the 3 calorimeter compartments. The electron energy is obtained by summing these four clusters after having applied weights to the presampler and to the back compartment energy to compensate for energy losses due respectively to dead material and to longitudinal leakage. Finally, the following effects, well reproduced in simulation data, are corrected: the lateral leakage caused by the finite cluster size, the  $\phi$  energy modulation caused by the accordion geometry, the residual dependence of the energy on the time between the particle arrival time and the phase of the sampling clock. The magnitude of each of these corrections is below 0.4%. For the end-cap energy the dependence on  $\eta$  due to the discrete high voltage settings (see Sect. 2) is also corrected.

### 3.2 Energy Resolution

Energy scans from 10 to 245 GeV have been performed at several positions. The distribution of the energy resolution as function of the beam energy  $E$  is found in good agreement with simulation. After unfolding the noise and the beam energy uncertainty (0.15%), the experimental points at a fixed position are well represented by the expression:

$$\frac{\sigma(E)}{E} = \frac{a}{\sqrt{E(\text{GeV})}} \oplus b$$

where  $a$  is the stochastic term and  $b$  the constant term reflecting local non uniformities ('local' constant term). For the stochastic term the fit result gave in every tested barrel position a value below  $10 \sqrt{\text{GeV}} \%$  (12.5 % for the end-cap) and for the local constant term a value smaller than 0.3 %. These results fulfil the ATLAS requirements which have been tuned on a few simulated benchmark channels like  $H \rightarrow 2\gamma$ ,  $H \rightarrow 2e^+2e^-$ ,  $W, Z$  decays [5]. If the contribution of the noise to the energy resolution is not unfolded but obtained by fitting the previous expression after the addition of a noise term,  $c/E(\text{GeV})$ , the result ( $c=0.18 \text{ GeV}$  at  $\eta = 0.675$ ) is in agreement with the noise measured in pedestal runs.

### 3.3 Uniformity of the Energy Response

The physics program [1] aimed at ATLAS (in particular the search for  $H \rightarrow 2\gamma$  events) requires a constant term in the energy resolution of 0.7% or smaller over the full calorimeter acceptance. This 'global' constant term is determined by the uniformity of the detector response over the full calorimeter acceptance. The strategy to obtain a uniform response is described in detail in [1] and requires in particular that a constant term  $\leq 0.5 \%$  can be obtained over a calorimeter region of size  $\Delta\eta \times \Delta\phi = 0.2 \times 0.4$ . These regions will be then cross-calibrated by using  $Z \rightarrow e^+e^-$  events. The uniformity of the calorimeter response as a function of the electron impact point has been studied by performing position scans over the entire module at a fixed energy. Fig. 1 shows the reconstructed energy as function of  $\eta$  for different  $\phi$  positions. Each

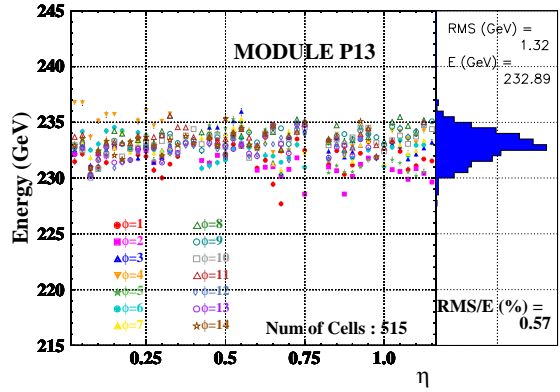


Fig. 1. Barrel module response as function of  $\eta$  and  $\phi$

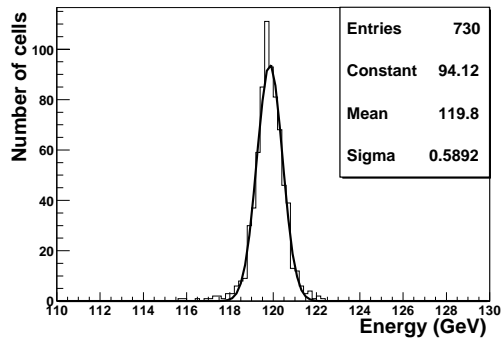


Fig. 2. Response uniformity of an end-cap module

point corresponds to the peak of the energy distribution of events impinging in one cell of the middle compartment. Therefore Fig. 1 describes the cell to cell variations for one of the tested modules. The region around  $\eta=0.8$ , corresponding to the transition between two different lead

thickness, is still being worked on and is not shown. The response dispersion is less than 0.6% both for the barrel and the end-cap modules (Fig. 2). As required, in regions of size  $\Delta\eta \times \Delta\phi = 0.2 \times (0.4 \text{ rad})$  the response dispersion is found smaller than 0.5%. The constant term of the energy resolution over a region  $\approx 6$  times bigger, corresponding to the entire module, can be obtained from the energy spectrum of the all electrons impinging on a module (Fig 3). The constant term for a module can be obtained from a Gaussian fit to this spectrum over the region not affected by the tail after unfolding the beam momentum spread, the measured sampling and noise term at a fixed position (see Sect. 3.2). The result is 0.70%, in agreement with the value obtained by adding the constant term  $b$  reflecting local non-uniformities (see Sect. 3.2) and the cell to cell variations (Fig. 1).

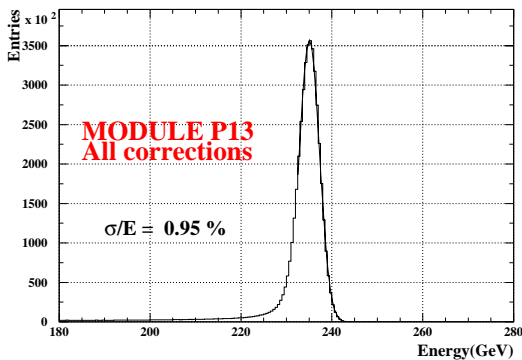


Fig. 3. Energy resolution for a whole barrel module

### 3.4 Position and Angular Resolution

Precise position and angular measurements play an important role in the reconstruction of the Higgs mass from the decay  $H \rightarrow 2\gamma$  and in the search for events with non pointing photons [1]. The shower positions in the front and middle compartment have been estimated as the energy weighted barycenters in each compartment corrected for the finite cell size. Using 245 GeV electrons, the shower position resolution was studied as function of  $\eta$  and, after unfolding the beam chamber resolution ( $250 \mu\text{m}$ ), the result was found in agreement with MC. In particular at small  $\eta$  the position resolution in the front and in the middle compartment was found to be  $240 \mu\text{m}$  and  $540 \mu\text{m}$ , respectively. Combining the position measurements in the front and in the middle compartment with the longitudinal shower barycenters the shower direction was computed. With this procedure the angular resolution on the shower axis measurement when using only informations from the calorimeter was found to be equal to  $50 \text{ mrad}/\sqrt{E(\text{GeV})}$  (Fig. 4). This result is within ATLAS requirements.

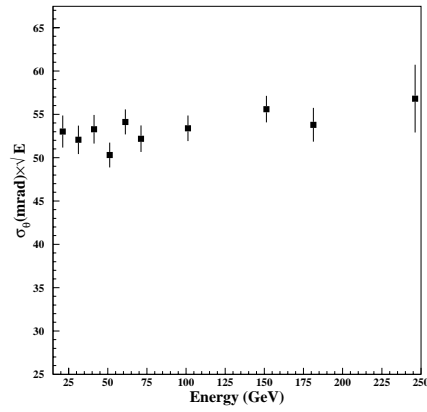


Fig. 4. Angular resolution versus the beam energy at  $\eta=0.68$

### 3.5 Time Resolution

Using the optimal filtering technique (see Sect. 3.1), the ATLAS electromagnetic calorimeter has the capability to measure the particle impact time [4]. A precise knowledge of the particle arrival time plays an important role in rejecting background events, like beam-gas events, and in searching for events with delayed photons with respect to the beam crossing. These photons would be produced by long lived neutralino decays in GMSB models[1]. By comparing for the same electron the time measurement in two adjacent cells, the time resolution as function of the energy of the most energetic cell has been measured and found to be better than 100 ps at all energies above 30 GeV. This result is well within ATLAS specifications.

## 4 Conclusions and Outlook

Significant parts of the calorimeter have been completed and the construction and assembly are on schedule. Test beam results from final modules indicate that the detector meets the very demanding requirements for the LHC physics. The next steps are combined test-beam measurements in 2004 including the Inner Detector, the electromagnetic and the hadronic calorimeter. The aim of these tests is to optimize the different components of the experiment in a situation very close to the ATLAS configuration.

## References

1. ATLAS Collab., *Detector and Physics Performances*, CERN/LHCC/99-15.
2. ATLAS Collab., *Liquid Argon Calorimeter Technical Design Report*, CERN/LHCC/96-41.
3. ATLAS Electromagnetic Liquid Argon Calorimeter Group, Nucl. Inst. Meth. **A 500**, (2003) 202.
4. ATLAS Electromagnetic Liquid Argon Calorimeter Group, Nucl. Inst. Meth. **A 500**, (2003) 178.
5. W.E. Cleland et al., Nucl. Instr. Meth. **A 338**, (1994) 467.
6. ATLAS Collab., *Calorimeter Performances Technical Design Report*, CERN/LHCC/96-40.